

## Optimal and Robust Tuning of State Feedback Controller for Rotary Inverted Pendulum

**Dr. Hazem I. Ali**

Control and Systems Engineering Department, University of Technology/Baghdad

Email: hazemcontrol2001@yahoo.com

**Rasha Mohammed Najji** 

Control and Systems Engineering Department, University of Technology/Baghdad

Email: rashaaliaya@gmail.com

Received on:30/3/2016 & Accepted on:20/10/2016

### ABSTRACT

This paper presents the design and implementation of optimal and robust state feedback controller for rotary inverted pendulum system. The Particle Swarm Optimization (PSO) method is used to find the optimal values of the state feedback gains subject to time response specifications and  $H_{\infty}$  constraints. To improve the tracking of the system, a robust state feedback plus integral controller is designed. The simulation results show that the proposed controller can effectively stabilize the pendulum at the upright position. Further, the proposed controller can compensate the variations in system parameters. The effectiveness of the proposed controller is verified experimentally using real rotary inverted pendulum.

**Keywords:** rotary inverted pendulum, robust controller,  $H_{\infty}$  control, state feedback controller

### INTRODUCTION

The rotary inverted pendulum system is widely used as a typical problem to study various modern control approaches. However, it is difficult to achieve precise control for such system because of this system is highly nonlinear, unstable, uncertain and multivariable system. Further, the rotary inverted pendulum is one of the under actuated systems where the system is driven by fewer numbers of actuators than its degree of freedom [1, 2].

The control of this system similar to different control systems exist in real time applications such as missiles and rockets, heavy crane lifting containers and self-balancing robots. According to the purposes, the control of the rotary inverted pendulum can be divided into three problems. The first is the problem of swing up the rotary inverted pendulum from the downward position to the upright position. The stabilization of the rotary inverted pendulum when it is in the upright position represents the second problem. The third problem is tracking control of the rotary inverted pendulum. On the other hand, the uncertainty in the rotary inverted pendulum systems makes it difficult to maintain good stability margins and performance properties for the closed loop system [2]. Therefore, a robust control is proposed to deal with the worst case design approach for a family of plants. Robust control is one of the main and important periods in control theory. Typically, it is required to design a controller to stabilize the plant if it is not originally stable and satisfies an acceptable level of performance with disturbance signals, noise interference, un modeled plant dynamics and plant parameter variations [3, 4].

On the other hand, many researches have been done in the field of controlling a rotary inverted pendulum system such as Ackhtaruzzaman and Shafie [5] that presented the design of classical control technique (2DOF) PID controller and modern control technique using Linear Quadratic Regulator (LQR). The experimental results showed that the 2DOF PID controller could maintain the inverted pendulum vertically up but it is not robust. Also, it was seen that the Linear Quadratic Regulator is more suitable to swing up the pendulum to its upright position and keep stability on the unstable equilibrium point. Tanaka et al. [6] validated the theoretical results obtained for swing up of the rotary inverted pendulum via a numerical simulation. Jadlovska and Sarnovsky [7] introduced stabilizing and swing up controllers for the rotary inverted pendulum system using full state feedback controller plus integral gain and LQR controller. Al-Jodah *et al.* [2] presented an experimental verification and comparison of different controllers for stabilizing the rotary inverted pendulum. An energy based method was used to swing up the inverted pendulum and to keep the pendulum in the upright position; a state feedback controller has been used. The mixed  $H_2/H_\infty$  state feedback controller was used to stabilize the pendulum. PD and Fuzzy PD controllers were presented by Oltean [8] for swing up and stabilizing the rotary inverted pendulum system. However, the system parameters uncertainty was not considered. Sukontanakarn and Parnichkun [9] proposed a swing up controller using energy based on PD controller and the stabilizing was achieved using LQR controller. However, no reference tracking has been considered and the robustness of the system was not investigated. A state feedback plus integral controller for stabilizing the rotary inverted pendulum system has been presented by Nundrakwang [10]. It was noted that the system parameters change was not considered in the design of the controller. An approach for the minimum time swing up of a rotary inverted pendulum using PD controller was proposed by Mary and Marimuthu [11]. The stabilizing controller was done using fuzzy balance controller.

A genetic algorithm was proposed by Kuo *et al.* [12] to find the optimal membership functions to the fuzzy logic controller to control the rotary inverted pendulum. The fuzzy logic controller adopted Gaussian-type input membership function, singleton output membership functions and center average defuzzification method. Chen and Huang [13] presented an adaptive controller to stabilize the rotary inverted pendulum with considering two parameters as uncertain parameters which are pendulum mass and center of gravity.

In this work the designs of robust state feedback and state feedback plus integral controllers are presented. To tune the state feedback gains, PSO method is used. These controllers can compensate the variations in system parameters. The effectiveness of the proposed controllers is verified experimentally using real rotary inverted pendulum.

The paper is organized as follows: The system mathematical model is given in Section 2. In Section 3, the design of the controller is presented. The simulation and experimental results are given in Section 4. In Section 5, the concluding remarks are presented.

### System Mathematical Model

The Quanser rotary inverted pendulum is used in this work as shown in Figure 1. Its components are horizontal arm attached to the load gear through a pivot and the other end has a bearing with a metal shaft. A T shape fitting is used to connect the pendulum to the shaft and it is free to rotate  $360^\circ$  perpendicular to the arm. The Quanser SRV02 rotary inverted pendulum has three sensors: tachometer, incremental encoder, and potentiometer. To measure the motor's angular position, the potentiometer and encoder are used while the tachometer is used to measure its angular velocity. The rotary inverted pendulum system is used in practice as a device with two degree of freedom represented by rotating arm and rotating pendulum rod therefore it is a Single –Input Multiple-

Output (SIMO) system [14]. The components of the rotary pendulum module are listed in Table 1 and labeled in Figure 2.



Figure (1) Quanser rotary inverted Pendulum

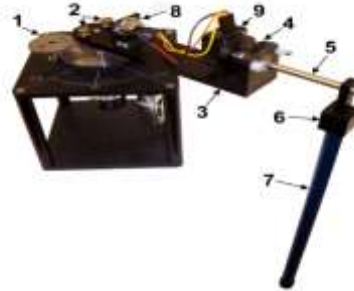


Figure (2) Rotary inverted pendulum components

Table(1). Listing of rotary inverted pendulum system components [14]

ID	1	2	3	4	5	6	7	8	9
Component	SRV02	Thumbscrews	Arm	Shaft Housing	Shaft	Pendulum T-Fitting	Pendulum link	Encoder Connector	Encoder

To develop the mathematical model for the rotary inverted pendulum, the top and front views of the rotary inverted pendulum are used as shown in Figures 3 and 4.

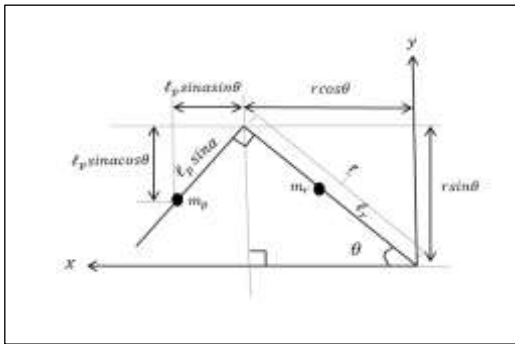
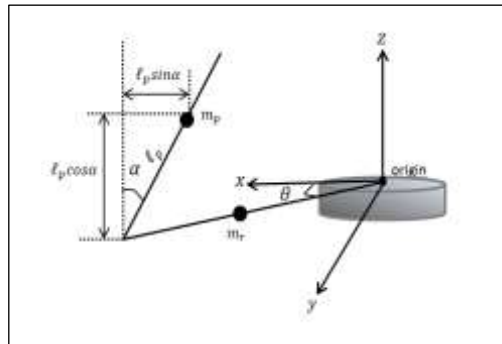


Figure (3) The top view of the rotary inverted system



Figure(4)The front view of the rotary pendulum.

The system origin is the center of the motor. The system coordinate is  $(xyz)$  using the standard Right Hand Cartesian. Looking at Figures 3 and 4, the following equations can be obtained [1]:

$$x_p = r \cos \theta - l_p \sin \alpha \sin \theta \quad \dots (1)$$

$$y_p = r \sin \theta + l_p \sin \alpha \cos \theta \quad \dots (2)$$

$$z_p = l_p \cos \alpha \quad \dots (3)$$

Where  $\theta$  is the rotation angle of pendulum arm and  $\alpha$  is the rotation angle of pendulum rod.  $\theta$  is positive when the pendulum arm rotating from  $x$  towards  $y$  and  $\alpha$  is positive when pendulum rod rotating from vertical position towards  $y$ . In other words  $\theta$  is positive counter clock wise (CCW) and  $\alpha$  is positive clock wise (CW). To obtain the square of the pendulum velocity, each axis will be differentiated and squared then combined as in the following equation:

$$v_p^2 = \dot{x}_p^2 + \dot{y}_p^2 + \dot{z}_p^2 \quad \dots(4)$$

Instead of using classical mechanics to obtain nonlinear equations of motion, the Lagrange method can be used to find the equation of motion of the system. This method is often used for more complicated systems.

In this work, the equations that describe the motions of the rotary arm and pendulum with respect to the dynamics  $(\theta, \alpha)$  are obtained using Lagrange method. The Lagrangian of the system is described by [12, 15]:

$$L = T_t - V \quad \dots(5)$$

Where  $T_t$  represents the total kinetic energy of the rotating body,  $V$  represents the total potential energy of the rotating body. Thus the Lagrangian is the difference between a system's kinetic and potential energies. By Euler-Lagrange equations explained in details in [2], the resulting rotary equations are:

$$(J_r + m_r \ell_r^2 + m_p L_r^2 + (J_p + m_p \ell_p^2) \sin^2 \alpha) \ddot{\theta} - (m_p L_r \ell_p \cos \alpha) \ddot{\alpha} + (B_r + (J_p + m_p \ell_p^2) \dot{\alpha} \sin \alpha \cos \alpha) \dot{\theta} + ((J_p + m_p \ell_p^2) \dot{\theta} \sin \alpha \cos \alpha + m_p L_r \ell_p \dot{\alpha} \sin \alpha) \dot{\alpha} = \tau \quad \dots (6)$$

$$-(m_p L_r \ell_p \cos \alpha) \ddot{\theta} + (J_p + m_p \ell_p^2) \ddot{\alpha} - ((J_p + m_p \ell_p^2) \dot{\theta} \sin \alpha \cos \alpha) \dot{\theta} + B_p \dot{\alpha} - m_p g \ell_p \sin \alpha = 0 \quad \dots (7)$$

The system parameters in these equations are given in Table 2.

To make the equation more compact, the following assumptions are considered:

$$\rho = J_r + m_r \ell_r^2 + m_p L_r^2, \quad \beta = J_p + m_p \ell_p^2, \quad \gamma = m_p L_r \ell_p, \quad \delta = m_p g \ell_p.$$

Equations (6) and (7) can be rewritten as [12]:

$$(\rho + \beta \sin^2 \alpha) \ddot{\theta} - (\gamma \cos \alpha) \ddot{\alpha} + (B_r + \beta \dot{\alpha} \sin \alpha \cos \alpha) \dot{\theta} + (\beta \dot{\theta} \sin \alpha \cos \alpha + \gamma \dot{\alpha} \sin \alpha) \dot{\alpha} = \tau \quad \dots (8)$$

$$-(\gamma \cos \alpha) \ddot{\theta} + \beta \ddot{\alpha} - (\beta \dot{\theta} \sin \alpha \cos \alpha) \dot{\theta} + B_p \dot{\alpha} - \delta \sin \alpha = 0 \quad \dots(9)$$

From Equation (8), it is shown that the motor torque equations are required and for more details about the motor equations, see reference [16]. The torque applied on  $\theta$  axis in Equation (8) is given by:

$$\tau = \frac{\eta_m \eta_g k_g k_t (V_m(t) - k_m k_g \omega_l(t))}{R_m} = \frac{\eta_m \eta_g k_g k_t (V_m(t) - k_m k_g \dot{\theta}(t))}{R_m} \quad \dots (10)$$

By substituting Equation (10) into Equation (8), the complete equations of the system after rearranging are [2]:

$$(\rho + \beta \sin^2 \alpha) \ddot{\theta} - (\gamma \cos \alpha) \ddot{\alpha} + \left( B_r + \beta \dot{\alpha} \sin \alpha \cos \alpha + \frac{\eta_m \eta_g k_m k_t k_g^2}{R_m} \right) \dot{\theta}$$

$$+(\beta \dot{\theta} \sin \alpha \cos \alpha + \gamma \dot{\alpha} \sin \alpha) \dot{\alpha} = \frac{\eta_m \eta_g k_g k_t V_m(t)}{R_m} \quad \dots(11)$$

$$-(\gamma \cos \alpha) \ddot{\theta} + \beta \ddot{\alpha} - (\beta \dot{\theta} \sin \alpha \cos \alpha) \dot{\theta} + B_p \dot{\alpha} - \delta \sin \alpha = 0 \quad \dots(12)$$

To find  $\ddot{\theta}$  and  $\ddot{\alpha}$  Equations (11) and (12) are to be solved. These equations can be written as [2]:

$$D(\theta, \alpha) \begin{pmatrix} \ddot{\theta} \\ \ddot{\alpha} \end{pmatrix} + C(\theta, \alpha, \dot{\theta}, \dot{\alpha}) \begin{pmatrix} \dot{\theta} \\ \dot{\alpha} \end{pmatrix} + G(\theta, \alpha) = HV_m(t) \quad \dots(13)$$

Where  $D(\theta, \alpha) = \begin{pmatrix} \rho + \beta \sin^2 \alpha & -\gamma \cos \alpha \\ -\gamma \cos \alpha & \beta \end{pmatrix}$ ,

$$C(\theta, \alpha, \dot{\theta}, \dot{\alpha}) = \begin{pmatrix} B_r + \beta \dot{\alpha} \sin \alpha \cos \alpha + \frac{\eta_m \eta_g k_m k_t k_g^2}{R_m} & \beta \dot{\theta} \sin \alpha \cos \alpha + \gamma \dot{\alpha} \sin \alpha \\ -\beta \dot{\theta} \sin \alpha \cos \alpha & B_p \end{pmatrix}$$

$$G(\theta, \alpha) = \begin{pmatrix} 0 \\ -\delta \sin \alpha \end{pmatrix}, H = \begin{pmatrix} \frac{\eta_m \eta_g k_g k_t}{R_m} \\ 0 \end{pmatrix}$$

where  $V_m$  is the motor input voltage.

The states  $\ddot{\theta}$  and  $\ddot{\alpha}$  are given by:

$$\begin{pmatrix} \ddot{\theta} \\ \ddot{\alpha} \end{pmatrix} = D^{-1}(\theta, \alpha) \left( HV_m(t) - C(\theta, \alpha, \dot{\theta}, \dot{\alpha}) \begin{pmatrix} \dot{\theta} \\ \dot{\alpha} \end{pmatrix} - G(\theta, \alpha) \right) \quad \dots(14)$$

By using Matlab's symbolic toolbox, the system of equations becomes:

$$\ddot{\theta} = \left( \frac{\eta_m \eta_g k_g k_t \beta V_m}{R_m} + \beta w - \beta B_r \dot{\theta} - \beta \gamma \dot{\alpha}^2 \sin \alpha + \delta \gamma \cos \alpha \sin \alpha + B_p \gamma \dot{\alpha} \cos \alpha + \beta \gamma \dot{\theta}^2 \cos^2 \alpha \sin \alpha - 2\beta^2 \dot{\alpha} \dot{\theta} \cos \alpha \sin \alpha - \frac{\eta_m \eta_g k_m k_t k_g^2 \beta \dot{\theta}}{R_m} \right) / (\beta^2 \sin^2 \alpha + \rho \beta - \gamma^2 \cos^2 \alpha) \dots (15)$$

$$\ddot{\alpha} = \left( \frac{\eta_m \eta_g k_g k_t \gamma \cos \alpha V_m(t)}{R_m} + \gamma \cos \alpha w - B_r \gamma \dot{\theta} \cos \alpha - \rho B_p \dot{\alpha} + \delta \rho \sin \alpha + \beta \delta \sin^3 \alpha - \beta B_p \dot{\alpha} \sin^2 \alpha + \beta^2 \dot{\theta}^2 \cos \alpha \sin^3 \alpha - \gamma^2 \dot{\alpha}^2 \cos \alpha \sin \alpha + \beta \rho \dot{\theta}^2 \cos \alpha \sin \alpha - 2\beta \gamma \dot{\alpha} \dot{\theta} \cos^2 \alpha \sin \alpha - \frac{\eta_m \eta_g k_g^2 k_m k_t \gamma \dot{\theta} \cos \alpha}{R_m} \right) / (\beta^2 \sin^2 \alpha + \rho \beta - \gamma^2 \cos^2 \alpha) \quad \dots(16)$$

The nonlinear system expressed by Equations (15) and (16) can be linearized as [13]:

$$\frac{dx}{dt} = f(x, V_m) \quad \text{and} \quad x = \begin{bmatrix} \theta \\ \dot{\theta} \\ \alpha \\ \dot{\alpha} \end{bmatrix} \quad \dots(17)$$

The Jacobian equation is used as follows [2, 17]:

$$\delta x' = A \delta x + B \delta V_m. \quad \dots (18)$$

Where

$$\delta x = X - X_0.$$

$$\delta V_m = V_m - V_{m0}.$$

The linearization around equilibrium point is defined as  $(X_0, V_{m0})$ :

$$X_0 = (\theta_0, \dot{\theta}_0, \alpha_0, \dot{\alpha}_0) = (0, 0, 0, 0).$$

$$V_{m0} = 0.$$

By Matlab, the following state space model is obtained:

$$\dot{x}(t) = \begin{bmatrix} 0 & 1 & 0 & 0 \\ 0 & \frac{\beta B_r}{R_m \gamma^2 - R_m \beta \rho} + \frac{\eta_m \eta_g K_g^2 K_m K_t \beta}{R_m \gamma^2 - R_m \beta \rho} & \frac{-\delta \gamma}{\gamma^2 - \beta \rho} & \frac{B_p \gamma}{\gamma^2 - \beta \rho} \\ 0 & 0 & 0 & 1 \\ 0 & \frac{\gamma B_r}{R_m \gamma^2 - R_m \beta \rho} + \frac{\eta_m \eta_g K_g^2 K_m K_t \gamma}{R_m \gamma^2 - R_m \beta \rho} & \frac{-\delta \rho}{\gamma^2 - \beta \rho} & \frac{B_p \rho}{\gamma^2 - \beta \rho} \end{bmatrix} x(t) + \begin{bmatrix} 0 \\ \frac{-\eta_m \eta_g K_g K_t \beta}{R_m \gamma^2 - R_m \beta \rho} \\ 0 \\ \frac{-\eta_m \eta_g K_g K_t \gamma}{R_m \gamma^2 - R_m \beta \rho} \end{bmatrix} u(t) \quad \dots (19)$$

$$y(t) = \begin{bmatrix} 1 & 0 & 0 & 0 \\ 0 & 0 & 1 & 0 \end{bmatrix} x(t) \quad \dots (20)$$

The parameters of system are given in Table 2.

**Table ( 2). Rotary inverted pendulum system parameters [14]**

Symbol	Description	Value	Unit
$R_m$	Armature resistance	2.6	$\Omega$
$B_{eq}$	viscous damping coefficient ( equivalent)	0.0150	N.m.s/rad
$J_{eq}$	moment of inertia ( equivalent)	0.003584179192918	Kg.m <sup>2</sup>
$k_g$	gear ratio	70	---
$k_m$	constant of back-emf	0.007677634454753	V.s/rad
$k_t$	torque constant (motor)	0.007682969729280	N.m/A
$\eta_g$	Efficiency of gearbox	0.9	---
$\eta_m$	Efficiency of motor	0.69	---
$L_p$	pendulum length	0.33655	m
$L_r$	arm length	0.2159	m
$\ell_p$	pendulum center of mass	0.155575	m
$\ell_r$	arm center of mass	0.0619125	m
$m_p$	pendulum mass	0.127	Kg
$m_r$	arm mass	0.257	Kg
$J_p$	pendulum moment of inertia	0.001198730801458	Kg.m <sup>2</sup>
$J_r$	moment of inertia about $\theta$ axis	9.98e-4	Kg.m <sup>2</sup>
$B_p$	viscous friction (pendulum rod joint)	0.0024	N.m.s/rad
$B_r$	viscous friction (arm joint)	0.0024	N.m.s/rad
$g$	Acceleration of gravity	9.81	m/s <sup>2</sup>

**Controller design**

The rotary inverted pendulum can be described by state space equations, this means that the state feedback, or pole placement can successfully stabilize the system. The desired closed loop poles are selected at the first step in the pole placement design. Further, the quadratic optimal control approach also may be used to find the desired closed loop poles of the system that it balances between the acceptable time response specifications and the amount of the required control energy [18, 19]. The tuning of the state feedback gain matrix is done using Particle Swarm Optimization (PSO) method based on a proposed cost function. The PSO is considered one of the high efficiency and effective optimization methods. It is inspired from studies of social behavior among ants and birds. For more details about PSO method, refer to [20, 21]. The position and velocity of each particle can be calculated by [20]:

$$x_{id}^{j+1} = x_{id}^j + v_{id}^{j+1} \dots (21)$$

$$v_{id}^{j+1} = w^j v_{id}^j + c_1 \cdot rand1(.) \cdot (p_{id}^j - x_{id}^j) + c_2 \cdot rand2(.) \cdot (p_{gd}^j - x_{gd}^j) \dots (22)$$

Where

$c_1$  and  $c_2$  represent positive constants.  $randi(.)$  are random numbers between 0 and 1,  $j$  is the iteration and  $d$  indicates elements in  $d^{th}$  dimension and  $w$  represents the inertia weight [18].

Consider an  $n^{th}$  -order system described by:

$$\dot{x}(t) = A x(t) + Bu(t) \dots (23)$$

Where

$x(t)$  represents the vector of states, and the scalar control law of the full state feedback (FSF)controller is [2]:

$$u(t) = -Kx(t) + e(t) \dots(24)$$

Where

$K$  represents constant gain elements and  $e(t)$  represents the error which defined by:

$$e(t) = \theta_{desired}(t) - \theta(t) = \theta_{desired}(t) - Cx(t) \dots(25)$$

The system ( $A, B$ ) is fully controllable if the matrix of the controllability ( $M$ ) has a full rank (rank must equal to 4 because the system is  $4^{th}$  order). The controllability matrix is [2, 13]:

$$M = [B \ AB \ A^2B \ A^3B] \dots(26)$$

The rank of the matrix  $M = 4$ , that is, the system is fully controllable and the closed loop model is represented by [2]:

$$\dot{x}(t) = (A - BK)x(t) + B\theta_{desired}(t), y(t) = Cx(t) \dots (27)$$

Since, the matrix  $A$  is controllable, by finding associated gain vector  $K$ , the closed loop state matrix  $A_{cl}$  or  $(A - BK)$  can be placed in any stable location  $s$ -plane. On the other hand, the presented state feedback controller has one deficiency in that it does not improve the system type and to solve this problem an integral control with state feedback is introduced. The control law of full state feedback plus integral (FSFI) controller is:

$$u(t) = K_I e(t) - K x(t) \dots(28)$$

The state error equation for the system with full state feedback plus integral control is defined by:

$$\hat{e}(t) = \theta_{desired}(t) - \theta(t) \quad \dots (29)$$

where

$$\hat{A} = \begin{bmatrix} A & 0 \\ -C & 0 \end{bmatrix}, \hat{B} = \begin{bmatrix} B \\ 0 \end{bmatrix}, \hat{e} = \begin{bmatrix} x \\ e \end{bmatrix} \quad \dots (30)$$

The rank of the controllability matrix  $M$  for Equation (30) to the system with full state feedback plus integral control is 5, which means that the system is completely state controllable. Then the arbitrary full state feedback controller design is possible. In this type of controller, the state feedback gain is:

$$\hat{K} = [K_1 \ K_2 \ K_3 \ K_4 \ ; \ K_I] \quad \dots (31)$$

To achieve more desirable transient response with the presence of uncertainty, the following cost function is proposed:

$$J_{min} = \int_0^{t_f} t|e(t)|dt + \int_0^{t_f} t|\alpha(t)|dt + \|W_p S + W_m T\|_{\infty} \quad \dots (32)$$

Where

$e(t)$  is the error between the actual output and the desired output,  $\alpha(t)$  represents the pendulum angle,  $t_f$  is the estimated settling time of the system,  $W_p$  is the performance weighting function,  $W_m$  is the Multiplicative uncertainty function,  $S$  is the Sensitivity function and  $T$  represents the Complementary sensitivity function. The performance specifications can be captured by the performance weighting function ( $W_p$ ) whose general form is selected as:

$$W_p(s) = \frac{a_n s^n + a_{n-1} s^{n-1} + \dots + a_0}{b_n s^n + b_{n-1} s^{n-1} + \dots + b_0} \quad \dots (33)$$

Where

$a$ 's and  $b$ 's are the coefficients of the performance weighting transfer function.

The multiplicative uncertainty model is expressed as [23]:

$$W_m(s) = \frac{G_i(s) - G_n(s)}{G_n(s)} \quad \dots (34)$$

Where

$G_i(s)$  represents perturbed plant at each value of uncertain parameters and  $G_n(s)$  is the nominal plant.  $W_m(s)$  is the upper bound of the frequency response obtained by applying equation (34) for variation parameters of the system.  $\Delta_m$  in Figures 5 and 6 will be equal to 1 and  $W_m(s)$  will be considered to represent the uncertainty.

To obtain a typical transfer function for  $W_m(s)$  from the upper bound frequency responses data, the Matlab commands "ginput" and "fitmag" are used to pick a set of upper bound frequency responses magnitudes and fit them to a stable transfer function. The resulting multiplicative uncertainty for 20% change in system parameters is:

$$W_m(s) = \frac{14.53s^7 + 380.1s^6 + 4344s^5 + 1.845 \times 10^4 s^4 + 1.69 \times 10^4 s^3 + 3926s^2 + 945.9s + 1.101}{s^7 + 19.25s^6 + 204.5s^5 + 616.3s^4 + 450.8s^3 + 106.7s^2 + 23.01s + 0.02683} \quad \dots (35)$$

The parameters that were applied to carry out the design of the controller using PSO method are: population size equal to 100, inertia weighting factor equal to 2,  $c_1 = 2$  and  $c_2 = 2$ , number of iterations 150. Figures 5 and 6 show the overall block diagrams of state feedback and state feedback

plus integral controllers tuned by PSO method, respectively. The proposed PSO algorithm can be described by the flowchart shown in Figure 7.

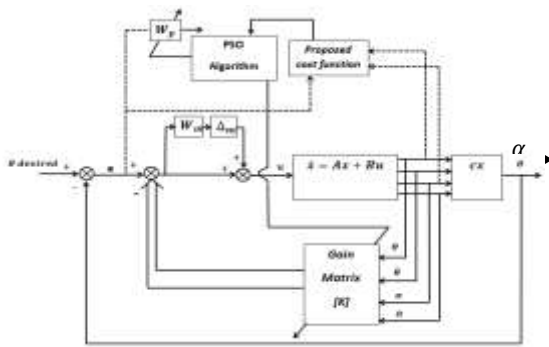


Figure ( 5): Block diagram of robust state feedback controller with PSO algorithm.

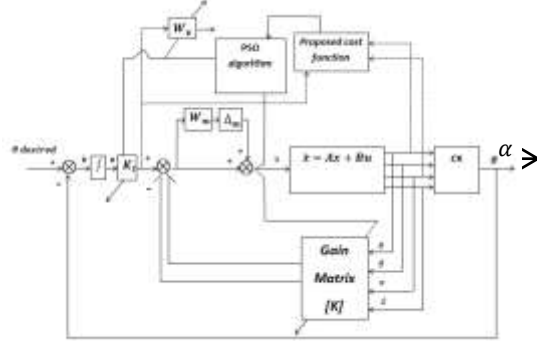


Figure ( 6): Block diagram of robust state feedback plus integral controller with PSO algorithm.

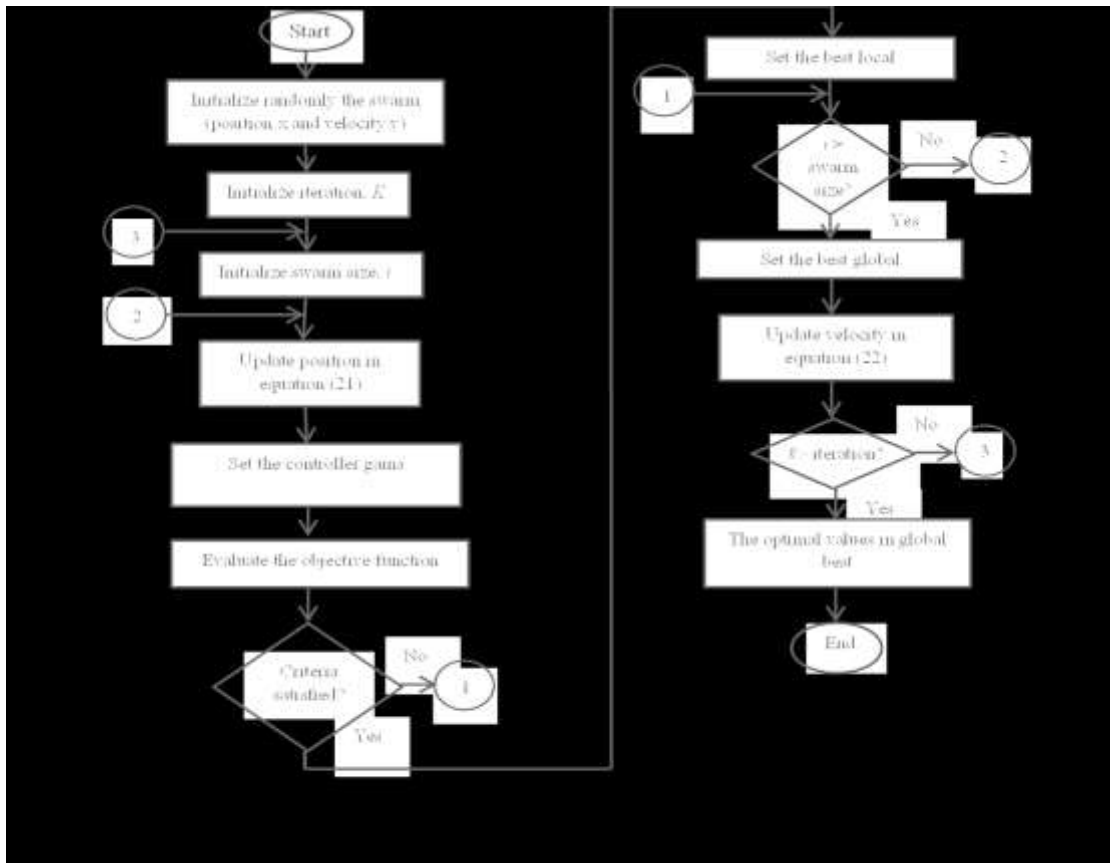
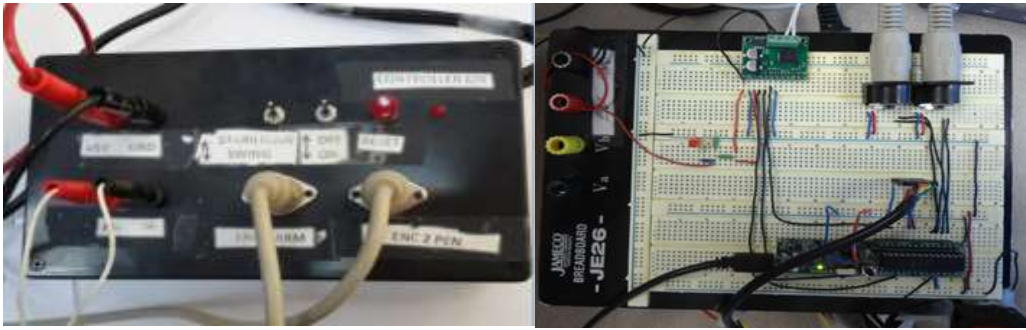


Figure (7). Flowchart of the proposed PSO algorithm

**System hardware implementation**

In this method, all controllers are embedded in the microcontroller with no need to the PC unless we decide to monitor the signals. The three controllers (swing up, stabilizing and switching controllers) are designed with Simulink and embedded target for Microchip®. Then the Simulink file is converted to C-code using Simulink coder. The C-code is compiled and converted to an equivalent assembly code using Microchip® C30 compiler. The generated program is downloaded to the microcontroller. Figure 8 shows the controller bread board of rotary inverted pendulum. Also Figure 9 shows the closer look of the controller bread board. As we can see the microcontroller on the bottom of the board, the two encoders connections on the top right, and the MC33926 motor driver carrier on the top left. The manual switch is provided to allow the experiment to be performed with manual swing up or stabilizing mode.



Figure( 8). The controller bread board      Figure (9). The controller bread board

A 20 KHZ PWM is used to control the average voltage delivered to the motor which is in the range, and the driver can handle this high frequency with minimal problems. The driver digital inputs are TTL compatible hence we do not need any conversion circuits. Figure 10 is a schematic layout of the experimental control system.

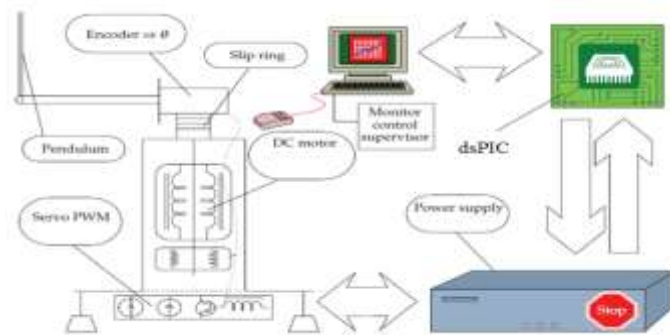


Figure (10): Schematic layout of the experimental control.

**Results And Discussion**

Figure 11 shows the time response of the system with robust full state feedback controller. The resulting gains are:  $k = [-4.05 \quad -2.67 \quad 27.27 \quad 4.99]$  and the time response specifications for arm angle are:  $t_r = 0.3847 \text{ sec}$ ,  $t_s = 1.9301 \text{ sec}$ ,  $M_p = 9\%$ , and for pendulum angle are:  $\alpha = -0.62$  to  $0.42$  degree and  $t_s = 2.4935 \text{ sec}$ .

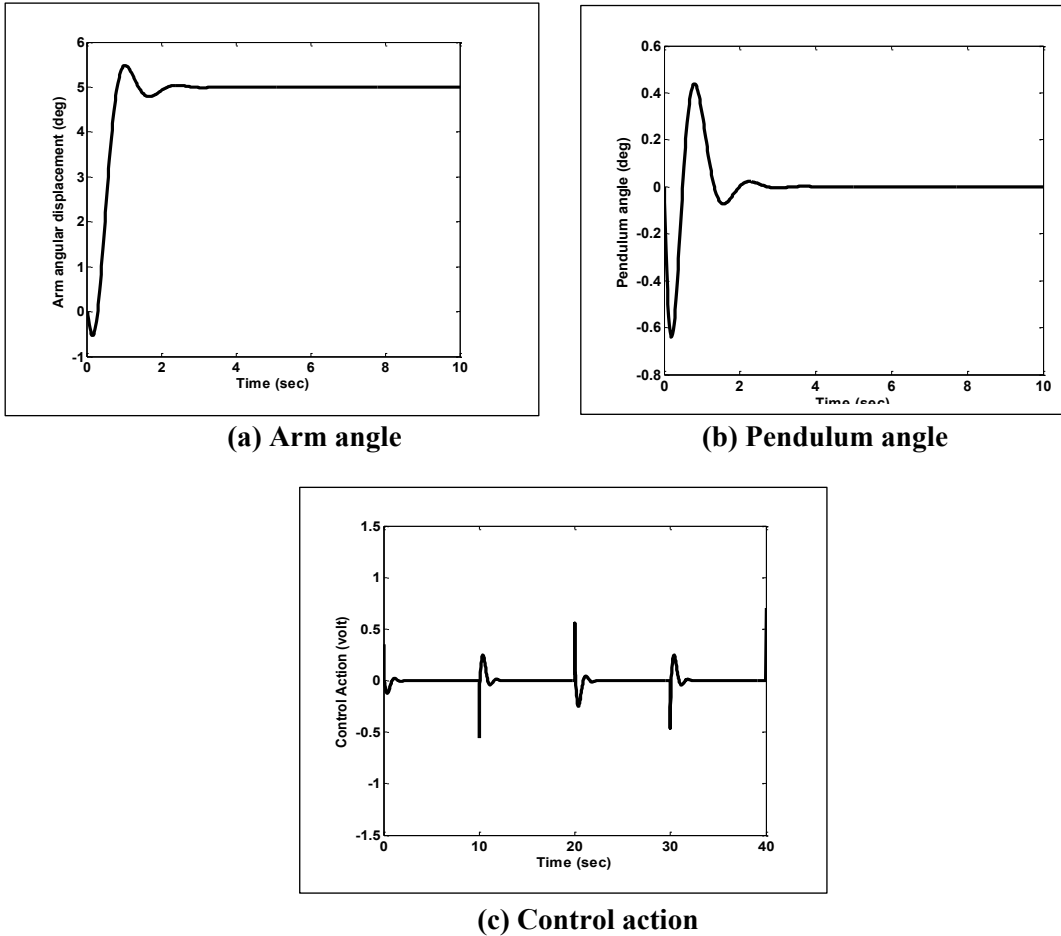
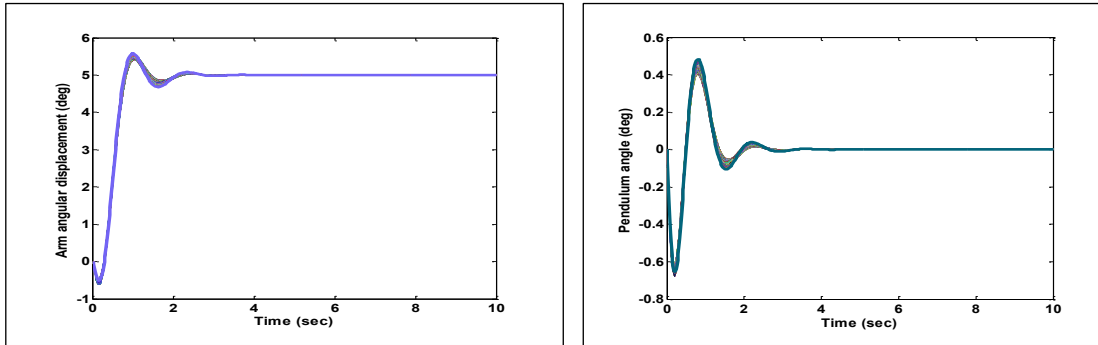


Figure (11) Controlled system time response specifications with robust FSF controller

To test the system robustness using the designed robust state feedback controller to the armature resistance ( $R_m$ ), mass of the arm ( $M_r$ ), mass of pendulum ( $M_p$ ), viscous friction on arm joint ( $B_r$ ), and viscous friction on pendulum rod joint ( $B_p$ ) are varied with 20%. Figure 12 shows the system response with uncertain parameters. It is shown that the system is stable despite the system parameters change. This means that the proposed robust state feedback controller can effectively compensate the variations in system parameters

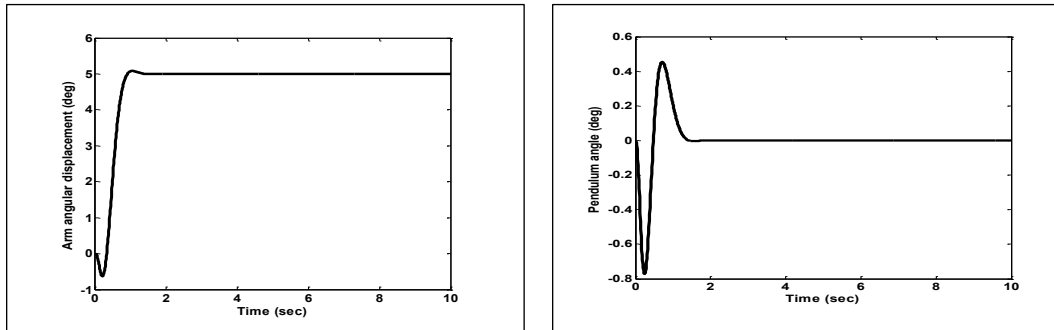


(a) Arm angle

(b) Pendulum angle

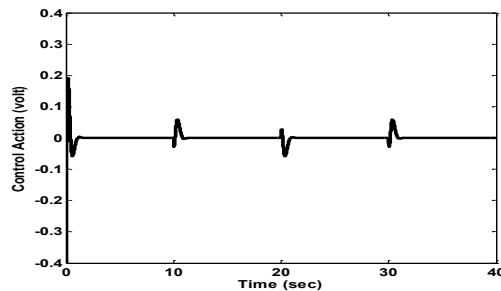
Figure (12): Uncertain controlled system time response specifications in case of robust FSF controller.

Figure 13 shows the time specifications of the system when the robust state feedback plus integral controller was applied. The obtained time response specification are:  $t_r = 0.3764 \text{ sec}$ ,  $t_s = 0.8458 \text{ sec}$ ,  $M_p = 1 \%$  for arm angle and  $\alpha = -0.77$  to  $0.45$  degree and  $t_s = 1.313 \text{ sec}$  for pendulum. The resulting gains are  $k = [-16.6886 \ -5.1963 \ 43.5277 \ 6.0893]$ ,  $K_I = -30]$ . The resulting control action is practically acceptable because its variations are within the limits of input voltage.



(a) Arm angle

(b) Pendulum angle



(c)Control action

Figure 13: Controlled system time response specifications with robust FSF plus integral controller.

On the other hand, to test the robustness, the time response of the uncertain system in case of robust FSF plus integral controller is shown in Figure 14. From this figure, it is shown that the proposed controller can effectively compensate the system parameter variations and satisfy the robustness. Further, it is shown that the responses of all uncertain plant members are very close to the nominal response. This means that the robust performance for the rotary inverted pendulum has been achieved entirely.

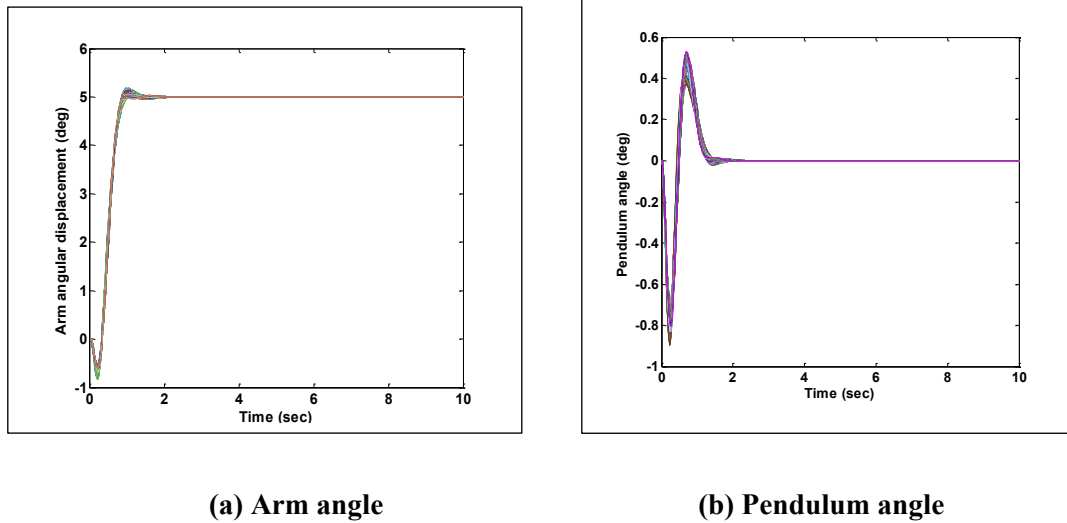


Figure (14): Controlled system time response specifications with uncertain parameters in case of robust FSF plus integral controller.

In the previous paragraphs, the results of applying the robust state feedback and robust state feedback plus integral controllers for rotary inverted pendulum were demonstrated. These results showed that the time response specifications obtained by robust state feedback plus integral controller are more desirable in comparison to those obtained by robust state feedback controller. Table 4 summarizes the results of the two robust controllers. It shows that the robust state feedback plus integral controller can yield a low control effort in addition to the desirable time response specifications.

Table( 4): Comparison between the performances of the two designed robust controllers.

Controller	Arm angle			Pendulum angle		
	$t_r$ (sec.)	$t_s$ (sec.)	$M_p$ %	$t_s$ (sec.)	$\alpha$ (deg.)	$V_m$ (volt)
Robust FSF	0.3847	1.9301	9	2.4935	-0.62 to 0.42	-0.5 to 0.5
Robust FSFI	0.3764	0.8458	1	1.313	-0.77 to 0.45	-0.05 to 0.05

The effectiveness of the proposed robust state feedback plus integral controller is shown by a comparison between its performance and performances of controllers designed in previous works which is given in Table 5. It shows that the transient response specifications achieved by the robust FSF plus integral controller are the best among the controllers in previous works.

Table (5): Performance comparison with previous works.

Controller	Arm angle			Pendulum angle	
	$t_r$ (sec.)	$t_s$ (sec.)	$t_s$ (sec.)	$\alpha$ (deg.)	$V_m$ (volt)
Fuzzy logic [12]	0.9	10	13	-0.5 to 0.4	-5 to 05
Fuzzy PD [8]	0.5	2	2	-10 to 18	-20 to 20
Proposed robust FSF plus integral	0.3764	0.8458	1.313	-0.77 to 0.45	-0.05 to 0.05

The experimental results of the swing up controller are shown in Figure 15. From these results, it is shown that the pendulum needs about 5 seconds for swinging from the downward position to the upright position within -3 to 3 degree. Figure 16 shows the resulting control action. The amplitudes of this control action are  $\mp 3$  volt which are within the limits of input voltages.

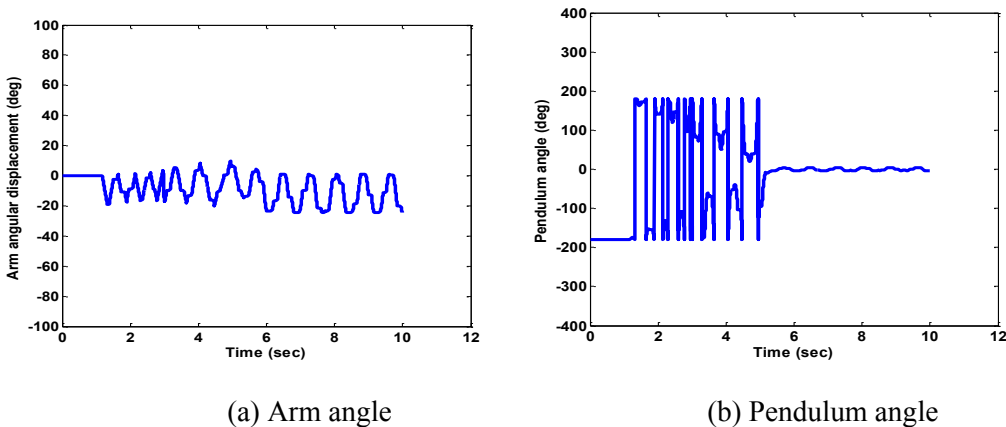
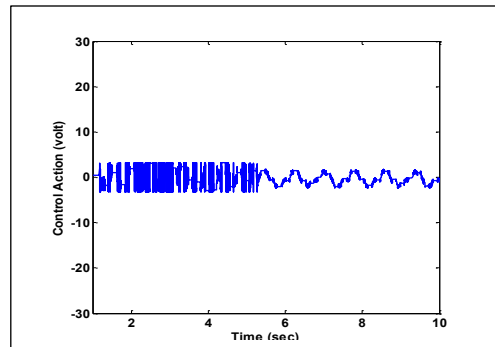
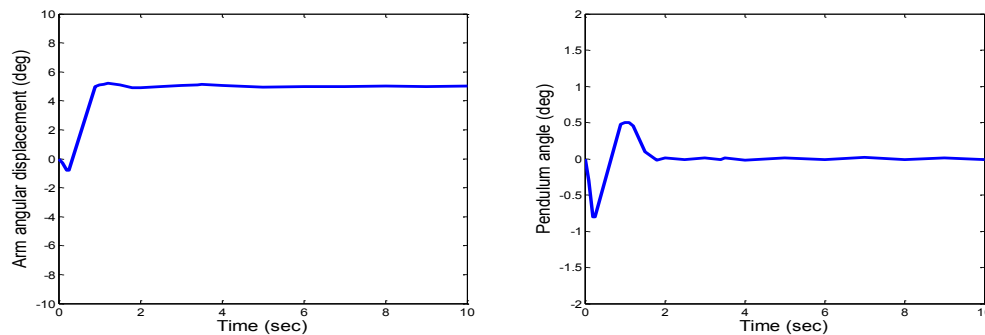


Figure (15): Swing up controller response (without FSF stabilizing controller).



**Figure (16): Response of the motor voltage in case of swing up controller.**

To show experimentally the effectiveness of the proposed controller, the robust FSF plus integral controller was applied to a real rotary inverted pendulum system explained in section 2. Figure 17 shows the experimental results. It is shown that the robust state feedback plus integral controller can stabilize the system with desirable time response specifications.

**Figure (17): Experimental time response specifications in case of robust FSF plus integral controller.**

## CONCLUSION

In this work, the designs of state feedback and state feedback plus integral controllers for rotary inverted pendulum system have been presented. The optimal values of the state feedback gains have been obtained using PSO method. To meet the robustness and time response specifications requirements, the time response specifications and  $H_{\infty}$  constraints were combined in the proposed cost function. The state feedback plus integral was designed to improve the system tracking. It was shown that the proposed robust FSF plus integral controller can effectively drive the system and the use of PSO method makes the controller computationally efficient. Furthermore, the time response specifications obtained by the robust FSF plus integral controller are more desirable in comparison to those obtained the robust FSF controller and the controllers designed in previous works. In addition, the variations in system parameters have been sufficiently compensated by the proposed FSF plus integral controller. Finally, the proposed robust FSF plus integral controller has been verified experimentally on the real rotary inverted pendulum system.

## REFERENCES

- [1] Acosta J. Á., "Furuta's Pendulum: A Conservative Nonlinear Model for Theory and Practice, Hindawi Publishing Corporation Mathematical Problems in Engineering, pp. 1-29, 2010.
- [2] Al- Jodah A., Zargarzadeh H. and Abbas M. K., "Experimental Verification and Comparison of Different Stabilizing Controllers for a Rotary Inverted Pendulum", IEEE International Conference on Control System, Computing and Engineering, Malaysia, pp.417-423, 2013.
- [3] Gu D.W., Petkov P. Hr., and Konstantinov M. M., "Robust Control Design with Matlab", Springer, 2005.
- [4] Dorf R. C. and Bishop R. H., "Modern Control Systems", Pearson Education, Inc., 2008.

- [5] Akhtaruzzaman M. and Shafie A. A., "Modeling and Control of a Rotary Inverted Pendulum using Various Methods, Comparative Assessment and Result Analysis", IEEE International Conference on Mechatronics and Automation, China, pp. 1342-1347, 2010.
- [6] Tanaka S., Xin X. and Yamasaki T., "Experimental Verification of Energy-Based Swing up Control for a Rotational Pendulum", SICE Annual conference, Japan, pp. 534-539, 2012.
- [7] Jadlovska, Slávka, and J. Sarnovsky. "Swingup and Stabilizing Control of Classical and Rotary Inverted Pendulum Systems." Proceeding of the 12th Scientific Conference of Young Researchers (SCYR 2012). Herlany: The Technical University of Kosice. 2012.
- [8] Oltean S., "Swing-up and Stabilization of the Rotational Inverted Pendulum using PD and Fuzzy- PD Controllers", Procedia Technology, Vol.12, pp. 57-64, 2014.
- [9] Sukontanakarn V. and Parnichkun M., "Real-Time Optimal Control for Rotary Inverted Pendulum", American Journal of Applied Sciences, Vol. 6, No. 6, pp. 1106-1114, 2009.
- [10] Nundrakwang S., Cahyadi A. I., Isarakorn D., Benjanarasuth T., Ngamwiwit J. and Komine N., "Swinging-up the Rotational Inverted Pendulum with Limited Sector of Arm Angle via Energy Control", ICCAS, Korea, 2005.
- [11] Mary P. M. and Marimuthu N. S. "Minimum Time Swing up and Stabilization of Rotary Inverted Pendulum using Pulse Step Control", Iranian Journal of Fuzzy systems, Vol. 6, No. 3, pp.1-15, 2009.
- [12] Kuo T., Huang Y. and Wu P., "Genetic Algorithm Tuned Fuzzy Logic Controller for Rotary Inverted Pendulum", Research Journal of Applied Sciences, Engineering and Technology, Vol. 6, No. 5, pp. 907-913, 2013.
- [13] Chen, Yung-Feng, and An-Chyau Huang. "Adaptive Control of Rotary Inverted Pendulum System with Time-Varying Uncertainties." Nonlinear Dynamics, Vol. 76, No. 1 pp. 95-102, 2014.
- [14] User Manual of ROTPEN.
- [15] Q. Inc., "Rotary Pendulum Workbook". 2011.
- [16] Xue D., Atherton D., and Chen Y., "Linear Feedback Control: Analysis and Design with MATLAB". 2007.
- [17] Faizan, F., Farid, F., Rehan, M., Mughal, S., and Qadri, M. T., "Implementation of Discrete PID on Inverted pendulum", 2nd International Conference on Education Technology and Computer (ICETC), IEEE, Vol. 1, pp. 48-51, 2010.
- [18] Yan Lan and MinruiFei, "Design of State-Feedback Controller by Pole Placement for a Coupled Set of Inverted Pendulums", 10<sup>th</sup> International Conference on Electronic Measurement and Instruments (ICEMI), Vol. 3, pp. 69-73, 2011.
- [19] Solihin, M. I. Akmeliawati, R., Tijani, I. B. and Legowo, A., "Robust State Feedback Controller Design via PSO Based Constrained Optimization", Control and Intelligent systems, Vol. 39, No.3, pp. 168-178, 2011.
- [20] Ali H. I. , Abbas Y. K. and Mahmood A. M. , "PSO Based PID Controller Design for a Precise Tracking of Two-Axis Piezoelectric Micro positioning Stage", Eng. & Tech. Journal, Vol. 3, Part (A), No. 17, pp. 2385-2397, 2013.
- [21] Ali H. I. "Robust PI-PD Controller Design for Magnetic Levitation System", Eng. & Tech. Journal, Vol. 32, No. 3, pp. 667-680, 2014.
- [22] Al-Waily R. S. A. and Al-Thuwainy A. A. K., "Designing Robust Mixed  $H_2/H_\infty$  PID Controllers Based Intelligent Genetic algorithm", Iraq J. Electrical and Electronic Engineering, Vol. 7, No.1, pp. 25-34, 2011.
- [23] Kemin Z. and Jhon D., "Essentials of Robust Control", Upper Saddle River, New Jersey: Prentice Hall Inc., 1998.